



Genetic structure, ecological versatility, and skull shape differentiation in *Arvicola* water voles (Rodentia, Cricetidae)

Pascale Chevret¹ | Sabrina Renaud¹ | Zeycan Helvacı² | Rainer G. Ulrich³ | Jean-Pierre Quéré⁴ | Johan R. Michaux^{2,5}

¹Laboratoire de Biométrie et Biologie Evolutive, UMR 5558, CNRS, Université Claude Bernard Lyon 1, Université de Lyon, Villeurbanne, France

²Conservation Genetics Laboratory, Institut de Botanique, Liège, Belgium

³Institute of Novel and Emerging Infectious Diseases, Friedrich-Loeffler-Institut, Federal Research Institute for Animal Health, Greifswald - Insel Riems, Germany

⁴Centre de Biologie et Gestion des Populations (INRA/IRD/Cirad/Montpellier SupAgro), Campus International de Baillarguet, Montpellier Cedex, France

⁵CIRAD/INRA UMR117 ASTRE, Campus International de Baillarguet, Montpellier Cedex, France

Correspondence

Pascale Chevret, Laboratoire de Biométrie et Biologie Evolutive, UMR 5558, CNRS, Université Claude Bernard Lyon 1, Université de Lyon, Villeurbanne, France. Email: pascale.chevret@univ-lyon1.fr

Present address

Zeycan Helvacı, Department of Biology, Aksaray University, Aksaray, Turkey

Funding information

FRS-FNRS grants, Belgian Fund for the Scientific Research

Abstract

Water voles from the genus *Arvicola* display an amazing ecological versatility, with aquatic and fossorial populations. The Southern water vole (*Arvicola sapidus*) is largely accepted as a valid species, as well as the newly described *Arvicola persicus*. In contrast, the taxonomic status and evolutionary relationships within *Arvicola amphibius* sensu lato had caused a long-standing debate. The phylogenetic relationships among *Arvicola* were reconstructed using the mitochondrial *cytochrome b* gene. Four lineages within *A. amphibius* s.l. were identified with good support: Western European, Eurasiatic, Italian, and Turkish lineages. Fossorial and aquatic forms were found together in all well-sampled lineages, evidencing that ecotypes do not correspond to distinct species. However, the Western European lineage mostly includes fossorial forms whereas the Eurasiatic lineage tends to include mostly aquatic forms. A morphometric analysis of skull shape evidenced a convergence of aquatic forms of the Eurasiatic lineage toward the typically aquatic shape of *A. sapidus*. The fossorial form of the Western European lineage, in contrast, displayed morphological adaptation to tooth-digging behavior, with expanded zygomatic arches and proodont incisors. Fossorial Eurasiatic forms displayed intermediate morphologies. This suggests a plastic component of skull shape variation, combined with a genetic component selected by the dominant ecology in each lineage. Integrating genetic distances and other biological data suggest that the Italian lineage may correspond to an incipient species (*Arvicola italicus*). The three other lineages most probably correspond to phylogeographic variations of a single species (*A. amphibius*), encompassing the former *A. amphibius*, *Arvicola terrestris*, *Arvicola scherman*, and *Arvicola monticola*.

KEYWORDS

Arvicola amphibius, *cytochrome b*, geometric morphometrics, phylogeography, plasticity

1 | INTRODUCTION

The extension of phylogeographical studies has led to the increasing recognition that many species traditionally identified based on

morphological traits encompass several genetic distinct forms that constitute “cryptic species” (e.g., Bryja et al., 2014; Mouton et al., 2017). Slow morphological divergence, as a probable consequence of stabilizing selection, may be responsible for the limited phenotypic

signature of these cryptic species. Yet, morphology, inclusive osteological traits, varies according to ecological conditions, including diet (Michaux, Chevret, & Renaud, 2007) but also way of life such as digging behavior, which exerts strong functional demands on the skull (Gomes Rodrigues, Šumbera, & Hautier, 2016). As a consequence, ecological versatility may lead to morphological convergence blurring the signature of genetic divergence between species. Assessing the evolutionary units involved in such cases is crucial to understand the selective context driving the genetic and morphological divergence.

Water voles of the genus *Arvicola* constitute an emblematic example of the controversies that may arise regarding ecological forms. Fossorial and semi-aquatic forms have been described as species (*Arvicola terrestris*, Linnaeus, 1758, type locality Uppsala, Sweden and *Arvicola amphibius*, Linnaeus, 1758, type locality England) already by Linnaeus in 1758. Later on, up to seven species have been described (Miller et al., 2012). By combining chromosomal and ecological data, only three species were thereafter proposed (Heim de Balsac & Guislain, 1955): the Southern water vole *Arvicola sapidus*, Miller, 1908, with $2n = 40$, *A. terrestris* for semi-aquatic forms with $2n = 36$, and *Arvicola scherman*, Shaw, 1801, for fossorial forms with $2n = 36$.

The status of *A. sapidus* was subject to little debate but controversy persisted regarding the aquatic and fossorial forms *A. terrestris/A. scherman*: considered as a single polytypic species (Wilson & Reeder, 1993), or valid distinct species: *A. amphibius* and *A. scherman* (Wilson & Reeder, 2005). More recently, the Italian water vole was proposed as a separate species (*Arvicola italicus*, Savi, 1839) (Castiglia et al., 2016), while the aquatic and fossorial forms remained considered as separate species with distinct geographic distribution, under the names of *A. amphibius* and *Arvicola monticola*, de Selys Longchamps, 1838 (Pardiñas et al., 2017). Even more recently, Mahmoudi et al. (2020) identified in Iran another species, *Arvicola persicus*, de Filippi, 1865. Hence, the genus *Arvicola* currently includes five species: *amphibius*, *italicus*, *monticola*, *sapidus*, and *persicus* (Mahmoudi et al., 2020; Pardiñas et al., 2017).

Yet, an increasing genetic sampling brought new fuel in the debate, showing that the ecological forms were not systematically associated with distinct clades. Fossorial and aquatic forms have been found to coexist in the Italian water vole (Castiglia et al., 2016) and in *A. scherman* (Kryštufek et al., 2015). The limited sampling of *A. monticola* precluded to reliably assess the variation in this presumed fossorial clade (Mahmoudi et al., 2020).

The present study therefore aims at a clarification of the phylogenetic pattern within European water voles, by compiling published and new *cytochrome b* sequences, with the aim to improve the geographic coverage and representation of the two ecological forms. This genetic approach was complemented by a morphometric analysis of skull shape variations of aquatic and fossorial forms, in order to assess the patterns of morphological differentiation and possible convergences.

2 | MATERIAL AND METHODS

The terminology used thereafter is the following. The Southern water vole, *A. sapidus*, and the Iranian water vole, *A. persicus*, were named by

their Latin name. The other water voles were designed as “water voles” or *A. amphibius* considered *sensu lato*, hence including both fossorial and aquatic water voles (including specimens labeled as *amphibius*, *monticola*, *scherman*, and *terrestris*). The status of the Italian water vole will be discussed, but the name “*italicus*” was tentatively retained.

2.1 | Material for genetics

The genetic sampling original to this study included 143 tissue samples of *A. amphibius* s.l. from Belgium, Denmark, France, Germany, Great Britain, and Spain, two specimens identified as *A. scherman* from Spain, as well as two samples of *A. sapidus* (Table S1). Most of the samples were attributed to fossorial or aquatic forms, based on field evidences: fossorial forms were trapped in tumuli. It was completed with sequences available in GenBank for *A. amphibius* (89), *A. scherman* (two), *A. sapidus* (12), and *A. persicus* (14) (Table S1). The complete dataset for *A. amphibius* s.l. comprised 236 sequences from 102 localities (Table S1, Figure 1a).

2.2 | Material for morphometrics

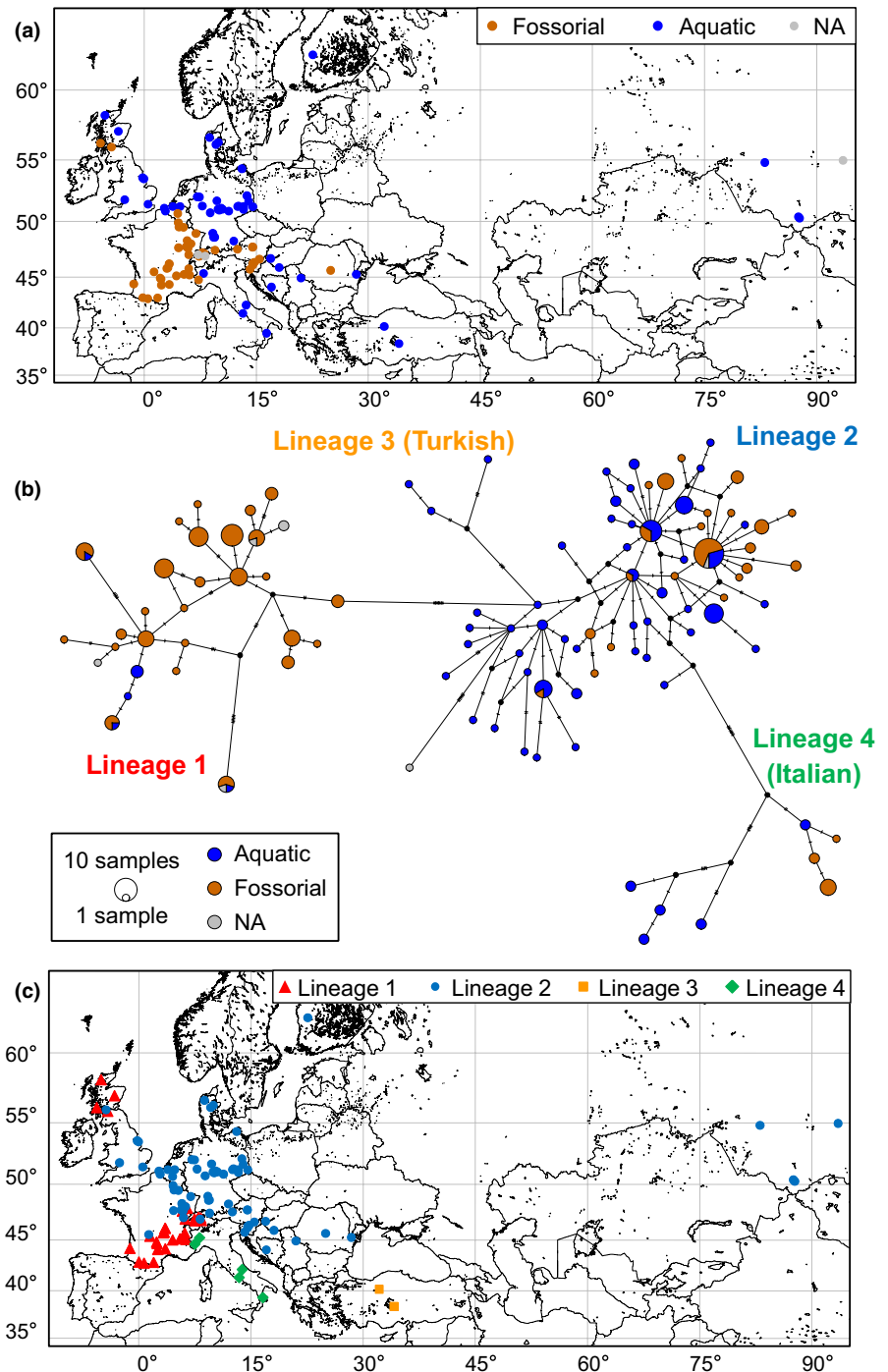
The material available for morphometric studies (Table S2) corresponded to 223 skulls. It included various fossorial populations from France and Western Switzerland. The Eurasiatic lineage (*sensu* Castiglia et al., 2016) was sampled by aquatic populations from Finland, Denmark, and Belgium. Water voles from Ticino in Southern Switzerland were labeled as *italicus* and represented the Italian lineage (Brace et al., 2016; Castiglia et al., 2016). Specimens from various localities in France and Spain represented the sister species *A. sapidus*.

In three populations (Chapelle d’Huin, La Grave, and Prangins), sex information was available and allowed to test for sexual dimorphism. Almost all specimens corresponded to adult and sub-adult specimens. The specimens are stored in the collections of the Centre de Biologie et Gestion des Populations (Baillarguet, Montferrier-sur-Lez, France), the Muséum d’Histoire Naturelle (Geneva, Switzerland), and the Université de Liège (Belgium).

2.3 | Genetic analysis

DNA was extracted from ethanol-preserved tissue of *Arvicola*, using the DNeasy Blood and Tissue kit (Qiagen) following the manufacturer instructions. The *cytochrome b* gene sequence was amplified using previously described primers L7 (5'-ACCAATGACATGAAAAATCATCGTT-3') and H6 (5'-TCTCCATTTCTGGTTTACAAGAC-3') (Montgelard, Bentz, Tirard, Verneau, & Catzeflis, 2002). PCRs were carried out in 50 μ l volume containing 12.5 μ l of each 2 mM primers, 1 μ l of 10 mM dNTP, 10 μ l of reaction buffer (Promega), 0.2 μ l of 5 U/ μ l Promega *Taq* DNA polymerase, and approximately 30 ng of DNA extract. Amplifications were performed using one activation step (94°C/4 min) followed by 40 cycles (94°C/30 s, 50°C/60 s, 72°C/90 s) with a final extension step at

FIGURE 1 Distribution of the ecological forms in the sampled localities (a), genetic network (b), and distribution of the genetic lineages (c)



72°C for 10 min. PCR products (1,243 bp long) were sent to Macrogen for sequencing.

The sequences generated were visualized and analyzed using Seqscape (Applied Biosystems) or CLC Workbench (Qiagen) and aligned with Seaview v4 (Gouy, Guindon, Gascuel, & Lyon, 2010). All the new sequences were submitted to GenBank: accession numbers LR746349–LR746495. The final alignment comprised 264 sequences of *Arvicola*, 147 new ones and 117 retrieved from GenBank. Sequences of *Microtus arvalis*, *Myodes glareolus*, *Eothenomys melanogaster*, and *Ellobius tancrei* were used as out-groups. This resulted in a final alignment comprising 268 sequences

and 911 positions (Alignment S1) after the removal of the sites with more than 10% of missing data. The best model fitting our data (GTR+I+G) were selected with jModelTest (Darriba, Taboada, Doallo, & Posada, 2012) using the Akaike criterion (Akaike, 1973). The phylogenetic tree was reconstructed using maximum likelihood with PhyML 3.0 (Guindon et al., 2010) and Bayesian inference with MrBayes v3.2 (Ronquist et al., 2012). Robustness of the nodes was estimated with 1,000 bootstrap replicates with PhyML and posterior probability with MrBayes. Markov chain Monte Carlo analyses were run independently for 20,000,000 generations with one tree sampled every 500 generations. The burn-in

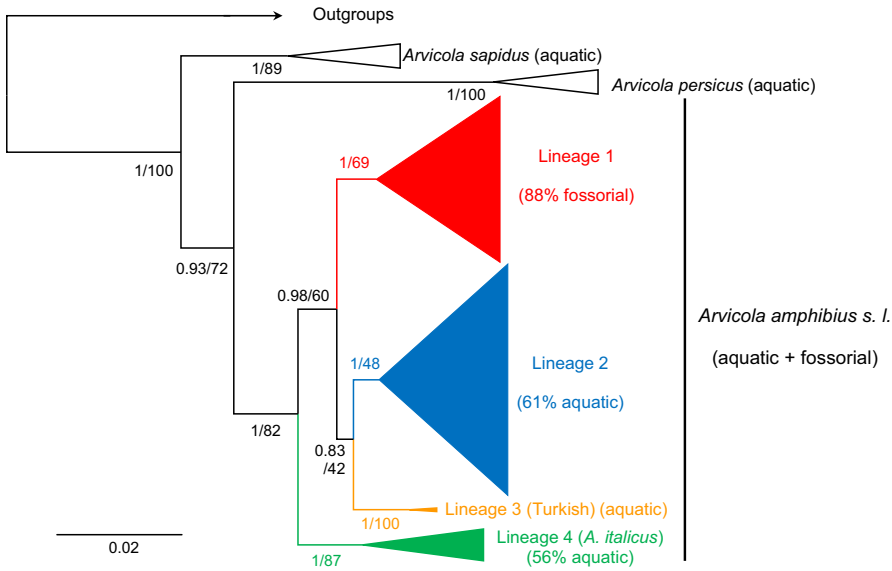


FIGURE 2 Simplified Bayesian phylogeny of *Arvicola* water voles. The support is indicated as follow: Posterior Probability (MrBayes)/Bootstrap Support (PhyML). The different lineages are indicated on the right side of the phylogeny. For each lineage, the dominant ecotype is indicated in brackets, with its percentage of occurrence based on the number of sequences in the tree attributed to this ecotype

was graphically determined with Tracer v1.6 (Rambaut, Suchard, Xie, & Drummond, 2014). We also checked that the effective sample sizes were above 200 and that the average standard deviation of split frequencies remained <0.05 after the burn-in threshold. We discarded 10% of the trees and visualized the resulting tree with Figtree v1.4 (Rambaut, 2012). MEGA 7 (Kumar, Stecher, & Tamura, 2016) was used to estimate K2P distance between and within lineages. We use POPART (Leigh & Bryant, 2015) to reconstruct a median-joining network of haplotypes (Bandelt, Forster, & Rohlf, 1999). This analysis was restricted to the 236 sequences of *A. amphibius*, and the corresponding haplotypes were determined with DnaSP v6 (Rozas et al., 2017).

2.4 | Morphometric analyses

Each skull was photographed in ventral and lateral views using a Canon EOS 400D digital camera. The ventral view was described by a configuration of 22 landmarks and 13 sliding semi-landmarks along the zygomatic arch. The lateral view was described using a configuration of 24 landmarks and 39 sliding semi-landmarks (Figure S1). All landmarks and sliding semi-landmarks were digitized using TPSdig2 (Rohlf, 2010). The sampling included 189 skulls in ventral view and 186 ones in lateral view (Table S2).

The configurations of landmarks and semi-landmarks were superimposed using a generalized Procrustes analysis standardizing size, position, and orientation while retaining the geometric relationships between specimens (Rohlf & Slice, 1990). During the superimposition, semi-landmarks were allowed sliding along their tangent vectors until their positions minimize the shape between specimens, the criterion being here bending energy (Bookstein, 1997). A principal component analysis (PCA) was performed on the resulting aligned coordinates. Relationships between different groups were investigated using a canonical variate analysis (CVA) which aims at separating groups by looking for linear combinations

of variables that maximize the between-group to within-group variance ratio. By standardizing within-group variance, this method may be efficient for evidencing phylogenetic relationships (Renaud, Dufour, Hardouin, Ledevin, & Auffray, 2015). In order to reduce the dimensionality of the data, the CVA was performed on the set of principal components (PC) totaling more than 95% of the variance.

Skull size was estimated using the centroid size (square root of the sum of the squared distances from each landmark to the centroid of the configuration). Size differences were tested using analyses of variance (ANOVA).

Geometric differences between groups and regression models were investigated using procedures adapted for Procrustes data (Procrustes ANOVA). Using this approach, the Procrustes distances among specimens are used to quantify explained and unexplained components of shape variation, which are statistically evaluated via permutation (here, 9,999 permutations) (Adams & Otárola-Castillo, 2013). Allometric variations were evaluated, investigating skull shape as a function of skull size. The effect of a grouping variable combining genetic and ecological information ("GxE") was also included (Table S2), allowing to test if the allometric slopes were different between the groups. Visualization was obtained using the common allometric component (CAC) derived from this allometry analysis (Adams, Rohlf & Slice, 2013). Procrustes superimposition, PCA, and Procrustes ANOVA were performed using the R package geomorph (Adams & Otárola-Castillo, 2013). The CVA was computed using the package Morpho (Schlager, 2017).

3 | RESULTS

3.1 | Genetics

On the phylogenetic tree (Figure 2, see Figure S2 for the complete phylogeny), the three groups corresponding to *A. sapidus*,

persicus, and *amphibius* s.l. were well supported (PP = 1, BP ≥ 82) with *A. amphibius* more closely related to *A. persicus* (PP = 0.93, PP = 72) than to *A. sapidus*. The phylogenetic tree as well as the network (Figure 1b) evidenced four lineages within *A. amphibius* s.l.. Most of the sequences of *amphibius* s.l. belonged to two lineages: Lineage 1 (L1) and Lineage 2 (L2). L1 was present in France, Spain, Switzerland, and the North of Great Britain and comprises mostly fossorial forms. This lineage was divided into two sub-groups: the first one with samples from France and Spain and the second one with samples from Great Britain, Switzerland, and France. The two specimens identified as *A. scherman* belonged to this lineage. L2 had a large repartition area from the south of Great Britain to Russia (East), Finland (North), and Romania (South) and it comprised more aquatic than fossorial forms. The two remaining lineages were restricted to Turkey, Lineage 3 (L3) with aquatic forms only and Italy, Lineage 4 (L4) with both aquatic and fossorial forms (Figure 2, Figure S2, and Figure 1c). In several French localities (Chapelle d'Huin, Doubs; Val d'Ajol, Vosges; Vauconcourt, Haute-Saône; Vigeois, Corrèze), a co-occurrence of lineages 1 and 2 was documented. In all cases, L1 was dominant and the population mostly fossorial.

Regarding the amount of genetic divergence, *A. sapidus*, *A. persicus*, and *A. amphibius* s.l. appeared well differentiated (K2P distances ≥ 7.2). L3 was closely related to L2 (K2P = 2.9) whereas L4, which correspond to *A. italicus*, was the most divergent (4.4 < K2P < 5.1) within *A. amphibius* s.l. (Table 1).

3.2 | Morphometrics

3.2.1 | Sexual dimorphism

Sexes displayed very similar skull size and shape. No difference was detected for the size of the skull in ventral view (ANOVA on Ventral Centroid Size: Chapelle d'Huin $p = .3031$; La Grave $p = .8706$; Prangins $p = .9799$) and in lateral view (ANOVA on Lateral Centroid Size: Chapelle d'Huin $p = .1358$; La Grave $p = .3575$; Prangins $p = .9576$). Similarly, skull shape was not different between sexes, for the skull in ventral view (Procrustes ANOVA on ventral skull shape: Chapelle d'Huin $p = .6130$; La Grave $p = .4556$; Prangins $p = .8309$) as for the skull in lateral view (Procrustes ANOVA on

lateral skull shape: Chapelle d'Huin $p = .1918$; La Grave $p = .4337$; Prangins $p = .7164$). All animals were therefore pooled in subsequent analyses.

3.2.2 | Skull size

The different groups of water voles significantly differed in skull size (ANOVA on CSventral and CSlateral: $p < .0001$). Skulls of water voles, being fossorial or aquatic, were smaller than those of *A. sapidus* (Figure 3). Important size variation occurred within *A. amphibius* s.l.. The aquatic populations of L2 were especially variable in size, the Belgian one being almost as large as *A. sapidus* whereas skulls from Finnish *A. amphibius* were among the smallest. Important size variation also occurred within populations belonging to L1.

3.2.3 | Skull shape in ventral view

The variation of skull shape in ventral view was structured in two groups on the first two axes of a PCA on the aligned coordinates (Figure 4a). These two groups opposed aquatic forms (*A. sapidus* and specimens belonging to L4 and L2) to fossorial forms belonging to L1. The L2 fossorial population from Alsace plotted between these two main groups, whereas the Slovakian specimens, presumably also belonging to L2 given the geographic extension of this lineage, plotted within the range of variation of fossorial L1. The fossorial specimens from Western Switzerland (Arzier and Prangins), presumably belonging to L1, and the population from Chappelle d'Huin, characterized by a genetic mixing of L1 and L2, shared the same range of variation as fossorial L1. The shape change from negative to positive PC1 scores, and hence from aquatic to fossorial forms, mostly involved a lateral extension of the zygomatic arch and a forward displacement of the incisor tip.

Both fossorial and aquatic groups displayed an important variation along PC1 and PC2. This was related to an important allometry (Figure 4b; Procrustes ANOVA on aligned coordinates: shape ~ CS: $p < .001$). A Procrustes ANOVA including as factors centroid size and the GxE grouping indicated a significant influence of both factors ($p < .001$) but supported the hypothesis of parallel slopes. These

TABLE 1 K2P distances and standard error between (below the diagonal) and within (on the diagonal) lineages

	Lineage 1	Lineage2	Lineage 3	Lineage 4	<i>Arvicola sapidus</i>	<i>Arvicola persicus</i>	Outgroup
Lineage 1	1.3 ± 0.2						
Lineage 2	4.1 ± 0.6	1.2 ± 0.2					
Lineage 3	3.8 ± 0.6	2.9 ± 0.5	0.6 ± 0.2				
Lineage 4	5.1 ± 0.8	4.4 ± 0.7	4.8 ± 0.8	1.6 ± 0.3			
<i>Arvicola sapidus</i>	7.5 ± 1.0	7.2 ± 0.9	7.6 ± 1.0	8.1 ± 1.1	0.9 ± 0.2		
<i>Arvicola persicus</i>	9.4 ± 1.2	10.1 ± 1.2	9.8 ± 1.2	9.2 ± 1.1	10.0 ± 1.2	1.2 ± 0.3	
Outgroup	19.2 ± 1.5	18.5 ± 1.4	18.3 ± 1.5	17.5 ± 1.5	17.8 ± 1.4	19.0 ± 1.5	17.2 ± 1.4

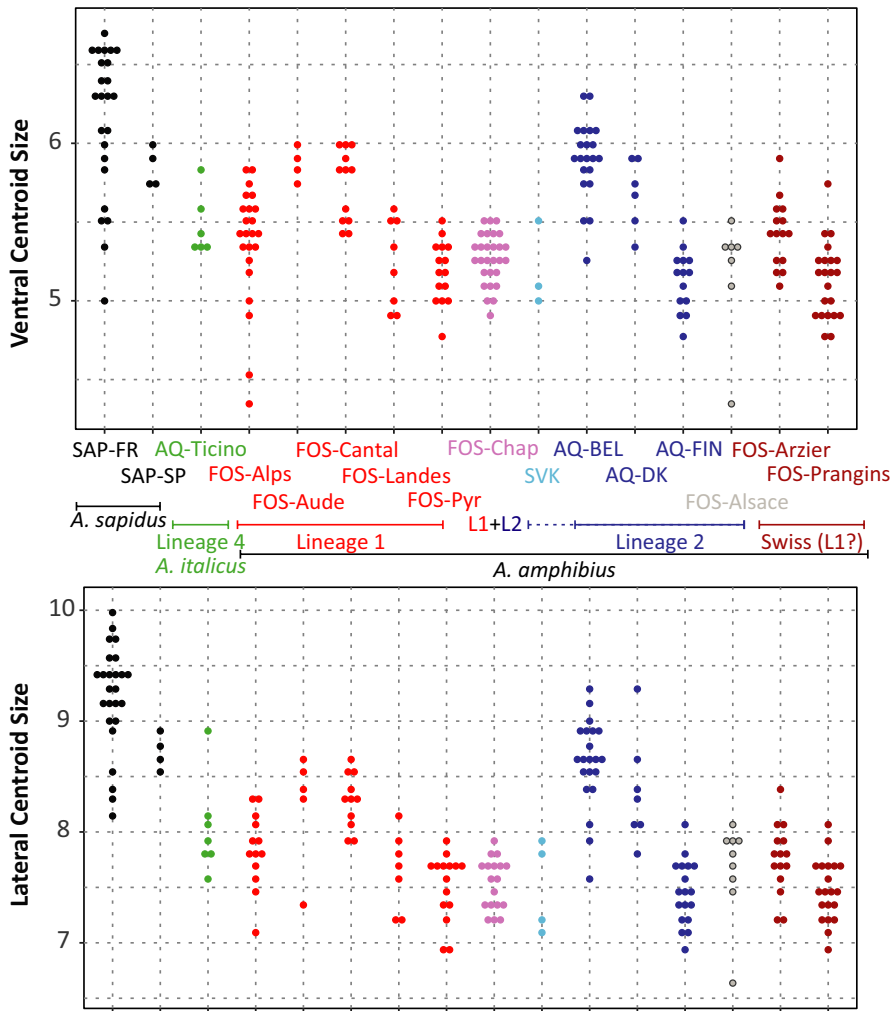


FIGURE 3 Variation of skull centroid size between populations of water voles (above, ventral side; bottom, lateral side). Each dot represents a specimen

parallel trends in the different groups were visualized along the CAC (Figure 4b), which involved discrete shape changes with a slight backward shift of the incisor tip, and a compression of the posterior part of zygomatic arch (Figure 4c). For similar CAC scores, aquatic forms tended to display larger skulls, especially those of *A. sapidus*.

The PCA on the aligned coordinates was further used to reduce the dimensionality of the data. The first 23 axes totaled 95% of the total variance and were used in a CVA, the grouping factors being the geographical groups (Figure 4d). As the PCA, the CVA tended to separate aquatic and fossorial forms; but it more clearly isolated *A. sapidus* and to a lesser extent the population from Ticino corresponding to the genetically well-differentiated L4. Despite their ecological heterogeneity, populations affiliated to L2, including the fossorial population from Alsace and the Slovakian population of unknown ecology, tended to share negative CVA1 scores. All other fossorial populations, affiliated to L1 or with a mixing of L1 and L2, plotted toward positive CVA1 scores.

The morphological differences between some groups means were further visualized (Figure 4c). The change from the aquatic *A. sapidus* to the typical fossorial water voles from the L1 mostly involved a lateral expansion of the zygomatic arch, a posteriorly compressed brain case and a forward shift of the incisor tip. The

lateral expansion of the zygomatic arch is also observed in the shape change from aquatic to fossorial ecology within L2. This change within L2 is, however, of a lesser magnitude than the change between the well-differentiated units *A. sapidus* and fossorial L1.

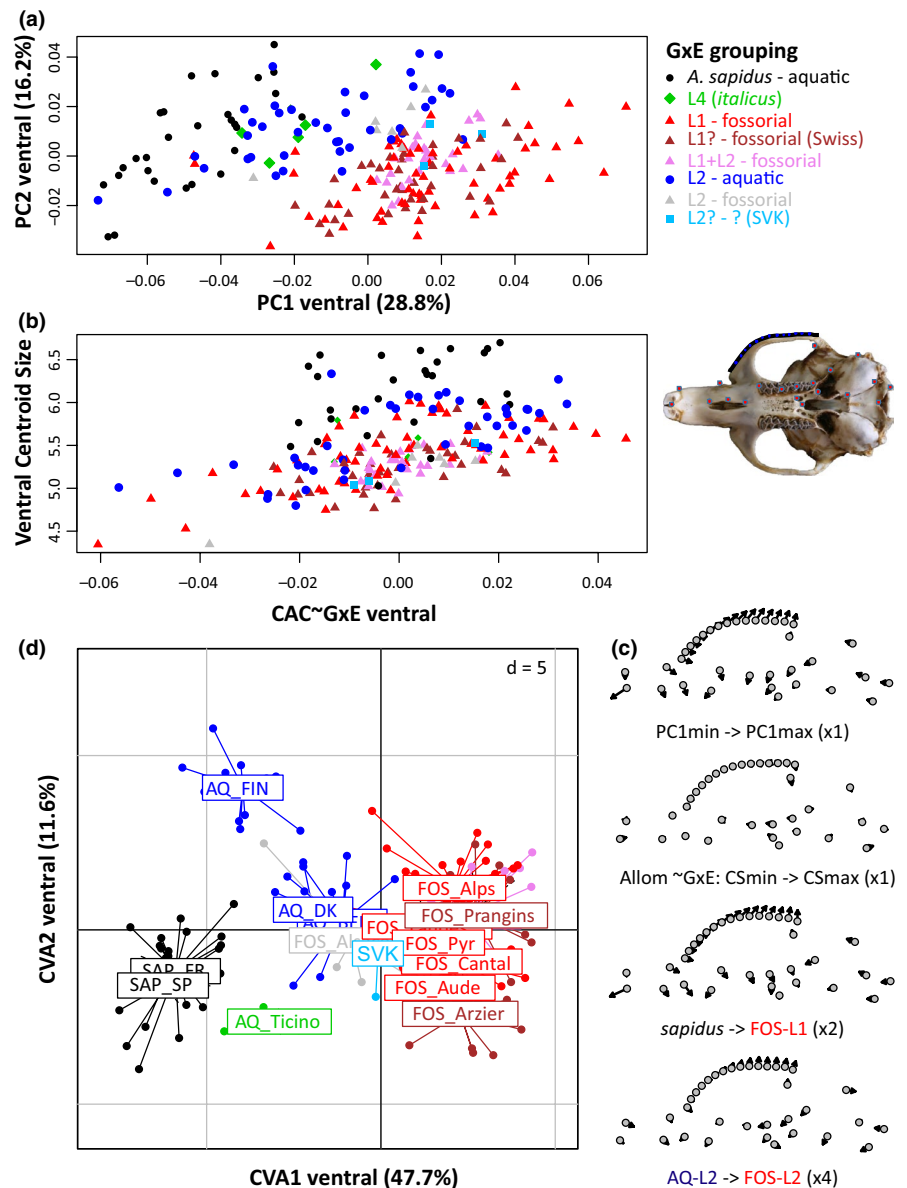
3.2.4 | Skull shape in lateral view

The PCA on the aligned coordinates of the skull in lateral view (Figure 5a) provided a less clear structure than the one of the skull in ventral view. Aquatic and fossorial forms tended to segregate along PC1, but with a considerable overlap. The shape changes along this axis involved a proodont shift of the incisor, a ventral expansion of the zygomatic arch, and a curvature of the brain case, but these shape changes corresponded both to a difference between aquatic and fossorial forms, and to an extensive variation within each ecological form.

This extensive variation is largely due to allometry (Procrustes ANOVA: shape ~ CS: $p < .001$). As for the ventral view, the different groups had parallel allometric slopes which were shifted between groups (Figure 5b; shape ~ CS: $p < .001$, ~ GxE: $p < .001$). The common allometric trend corresponded to a flattening of the brain case and a slight backward shift of the incisor tip (Figure 5c).

FIGURE 4 Skull shape in ventral view.

(a) Morphospace corresponding to the first two axes of a PCA on the aligned coordinates. (b) Allometric relationship, represented by the Common Allometric Component in the "GxE" groups (CAC_{GxE}), as a function of centroid size. (c) Visualization of shape changes, as arrows pointing from a first to a second item. From top to bottom: Shape changes along the first PC axis; allometric shape change, from minimum to maximum centroid size along the CAC_{GxE} ; change between the mean morphology of *Arvicola sapidus* and fossorial lineage 1; change between the mean morphology of aquatic and fossorial forms within lineage 2. (d) Morphospace corresponding to the first two axes of a CVA on the PC axes totaling 95% of shape variance



The first 29 axes of the PCA totaled 95% of variance and were used in a CVA (Figure 5d). *Arvicola sapidus* and the Ticino population from L4 appeared as well divergent along the first CVA axis, explaining most of the variation. All other populations were close to each other. Whatever their ecology, populations attributed to L2, including that from Slovakia, were tightly clustered toward CVA1 scores close to zero. All fossorial populations belonging to L1, or where lineages 1 and 2 co-occur, were clustered toward negative CVA1 scores.

The shape change between aquatic and fossorial group means (Figure 5c) allowed to better assess the shape changes related to ecology. The difference between *A. sapidus* and the fossorial L1 clearly showed the proodont shift of the incisor. This shift is also characteristic, although at a lesser magnitude, in the transition from aquatic to fossorial forms within L2; this was associated with a downward shift of the zygomatic arch.

4 | DISCUSSION

4.1 | Phylogeny evidenced widespread ecological versatility

The molecular data confirmed the separation of *A. sapidus* and *A. persicus* and other water voles as in Mahmoudi et al. (2020). They further evidenced four lineages within the "European water vole" *A. amphibius* s.l.: (a) L1, with a Western European distribution (Castiglia et al., 2016) and a dominance of fossorial forms. This lineage was found mostly in France, the neighboring Western Switzerland, and in Northern areas of Great Britain. (b) A widespread Eurasiatic L2 (Castiglia et al., 2016; Kryštufek et al., 2015), present from Belgium and Germany to the West up to Eastern parts of Russia. This lineage showed a dominance of aquatic forms. Note that the co-occurrence of lineages 1 and 2 in Great Britain

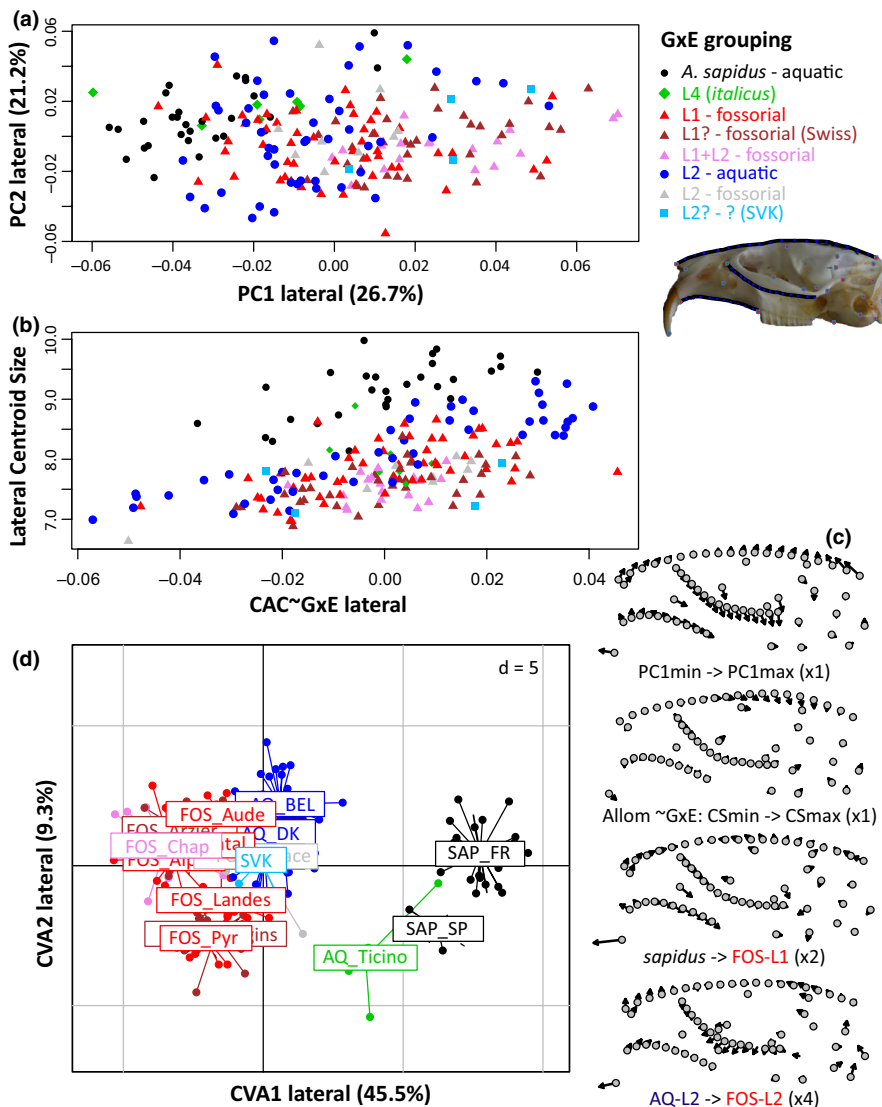


FIGURE 5 Skull shape in lateral view. (a) Morphospace corresponding to the first two axes of a PCA on the aligned coordinates. (b) Allometric relationship represented by the Common Allometric Component in the “GxE” groups (CAC_{GxE}), as a function of centroid size. (c) Visualization of shape changes, as arrows pointing from a first to a second item. From top to bottom: Shape changes along the first PC axis; allometric shape change, from minimum to maximum centroid size along the CAC_{GxE}; change between the mean morphology of *Arvicola sapidus* and fossorial lineage 1; change between the mean morphology of aquatic and fossorial forms within lineage 2. (d) Morphospace corresponding to the first two axes of a CVA on the PC axes totaling 95% of shape variance

has been shown to be the consequence of a colonization in two waves, the second partly replacing the first *ca* 12–8 kyr BP (Brace et al., 2016; Searle et al., 2009). (c) Related to the Eurasian L2, a third lineage (L3) was found, up to now, in Turkey (Kryštufek et al., 2015). (d) L4, characteristic of Italy and the neighboring Southern Switzerland (Ticino) (Brace et al., 2016; Castiglia et al., 2016). It was the most divergent of the lineages within *A. amphibius* s.l. and corresponded to the proposed species *A. italicus*.

Confirming recent results (Castiglia et al., 2016; Kryštufek et al., 2015), the present study undermined the interpretation of fossorial and aquatic forms as distinct genetic units. Instead, ecological versatility was evidenced within at least three out of four lineages, aquatic and fossorial forms being mixed in the lineages one (Western Europe), two (Eurasian), and four (Italian). The reduced sampling of L3 (Turkey) precluded any conclusions regarding this lineage. Clearly, aquatic and fossorial forms do not constitute separate species in water voles *A. amphibius* s.l. (Kryštufek et al., 2015).

The genetic distances separating the lineages fell within a “grey zone,” where values typical for intraspecific divergence and those associated with interspecific divergence overlap ($-3 < K2P < -6$)

(Barbosa, Pauperio, Searle, & Alves, 2013). With K2P values between 4 and 5, they typically corresponded to the range of differentiation between phylogenetic lineages within rodent species (Michaux, Magnanou, Paradis, Nieberding, & Libois, 2003; Paupério et al., 2012), and slightly below values corresponding to the differentiation between species (Amori, Gippoliti, & Castiglia, 2009; Kohli et al., 2014; Vallejo & González-Cózat, 2012).

4.2 | A twofold morphological signature

The morphological differentiation among water voles was assessed with two widely used methods in morphometrics: PCA and CVA. These methods provided different structures between populations in the corresponding morphospaces, the PCA emphasizing the morphological differences related to ecology, opposing aquatic, and fossorial voles whatever their phylogenetic background, while the CVA retrieved a signal more related to the phylogenetic structure. This discrepancy is related to the properties of the methods. The PCA decomposes the total variance and therefore is highly impacted by extensive

within-group variation related to ontogenetic and ecological changes. In contrast, by expressing between-group differences while standardizing within-group variance, the CVA can put forward more discrete traits characterizing different lineages. It is confirmed here as an efficient tool for showing phylogenetic relationships (Renaud et al., 2015).

4.3 | Ecological forms and their adaptive morphological signature on skull shape

The chisel-tooth digging behavior is known to exert strong physical loads on the skull, and thus to constitute a strong selective pressure leading to morphological convergence in skull shape across different rodent families (Gomes Rodrigues et al., 2016; Samuels & Van Valkenburgh, 2009). Accordingly, an important skull shape differentiation opposed aquatic to fossorial groups. Chisel-tooth digging especially requires powerful masseter muscles to move the mandible into occlusion. This muscle originates along the zygomatic arch and inserts on the angular process of the mandible. As a consequence, the expanded zygomatic arch is typical for fossorial rodents (Samuels & Van Valkenburgh, 2009). Proodont incisors are also a typical trait for fossorial rodents, favoring the process of biting in the substrate (Samuels & Van Valkenburgh, 2009). The signal found in *Arvicola* skulls agrees with these general ecomorphological characteristics: fossorial populations display an expanded angular processes on the mandible (Durão, Ventura, & Muñoz-Muñoz, 2019), and for the skull, an expansion of the zygomatic arch, especially visible in ventral view, and proodont incisors, a trait that is best traced in lateral view. Altogether, the morphometric differentiation between fossorial and aquatic water voles documents an integrated adaptive response to the functional demand of tooth digging.

Opposite to fossorial water voles, the skulls of *A. sapidus* display extreme skull shapes, without overlap with other water vole populations, even aquatic ones. This pronounced morphological differentiation (Durão et al., 2019; this study) is likely the combined result of a genetic divergence supportive of a valid species, and of the absence of ecological versatility in this taxon, always displaying a semi-aquatic way of life.

Within *A. amphibius* s.l., fossorial and aquatic populations tended to be well differentiated. This was especially true for the fossorial populations of the Western European L1 (dominantly fossorial) and the aquatic populations of the Eurasiatic L2 (mostly aquatic). The Alsacian fossorial population of L2 was shifted toward the fossorial populations of L1, but still displayed an intermediate morphology between aquatic and fossorial forms. This suggests that the genetic divergence between the two lineages was enough to accumulate adaptations to the dominant ecology. However, the persistent ecological versatility triggers local adaptation in case of a switch to the alternative strategy. This response in skull shape probably includes a plastic component, since bone permanently remodel in response to mechanical stress produced by muscular activity, including in the context of digging activity (Durão et al., 2019; Ventura & Casado-Cruz, 2011).

Regarding size, fossorial forms of *A. amphibius* s.l. were mentioned to be smaller than the aquatic forms in the Eurasiatic region (Kryštufek et al., 2015) but the reverse in Italy (Castiglia et al., 2016). The present study did not evidence any clear trend between lineages or forms, to the exceptions of the clearly larger *A. sapidus*. The hypothesis that burrowing would favor small-sized animals, because of reduced digging costs (Durão et al., 2019) is therefore not supported within *A. amphibius* s.l., although local ecological conditions may be involved in the important geographic differences in skull size even within the same lineage. The age structure of the sampled populations may explain at least partly differences in the size distribution, depending whether or not young animals were dominant at the time of trapping (Renaud, Hardouin, Quéré, & Chevret, 2017). Whatever its cause, size variation was associated with allometric variation of skull shape. *Arvicola sapidus*, and fossorial and aquatic forms of *A. amphibius* s.l. shared parallel allometric trajectories, fossorial forms showing more “adult-like” morphologies than aquatic ones for a given size. In that respect, the evolution of fossorial forms may be seen as heterochronic (Cubo, Ventura, & Casinos, 2006). However, the morphological signal directly related to allometry was of limited amount and did not match the differences related to ecology. Adaptive and plastic response to the functional demand of chisel-tooth digging thus appears a more likely explanation of the morphological differences between groups. The corresponding morphological characteristics seem to appear early in life, with a conservation of the ontogenetic trajectory in aquatic and fossorial water voles.

4.4 | Fossorial versus aquatic: an oversimplified classification

The Italian lineage (L4) was represented in the morphometric study by a sole population from Ticino in Switzerland. This population was within the range of aquatic populations in PCA morphospaces, in agreement with its dominant ecology. In the CVA morphospaces, it clearly departed from the other lineages of *A. amphibius* s.l., suggesting a morphological signature of the Italian lineage.

Similarly, populations belonging to L2 appeared clustered in the CVA plots, especially in lateral view, suggesting a morphological signature for this lineage as well. However, in the PCA morphospaces, these populations ranged from a typically aquatic to a fossorial morphology (considering the Slovakian population as likely belonging to this lineage), with the Alsacian population being intermediate in shape. This illustrates the ecological versatility of water voles when facing environmental changes. Furthermore, if some forms are attached all year to water, and some inhabit dry areas, some animals switch between both habitats during the year (Wust-Saucy, 1998). In front of this ecological versatility even on very short time scales, the expectation of discrete fossorial and aquatic morphotypes may be inadequate (Kryštufek et al., 2015). Typical aquatic voles from the dominantly aquatic L2 and typical fossorial voles from L1 might represent endmembers of a phenotypic continuum, the skull

morphology being dependent both on the genetic background and the ecological conditions of growth.

4.5 | Taxonomic implications

The strength of the present study relies on the extensive sampling of water voles across Europe. However, the taxonomic conclusions are only based on a mitochondrial gene (*cytochrome b*) and the pattern of morphological divergence of the skull. Nuclear data would be required to validate these conclusions, but the only data available so far, based on the *Interphotoreceptor Retinoid Binding Protein* gene, remained inconclusive for *A. amphibius* s.l. (Mahmoudi et al., 2020).

In agreement with previous studies, genetic and morphometric results support the specific status for the Southern water vole *A. sapidus* (type locality Santo Domingo de Silos, Burgos Province, Spain). Its genetic divergence from the other lineages ($K2P > 7$) was close to what is observed between other valid rodent species (Amori et al., 2009; Barbosa et al., 2013). The genetic divergence was also very high for the species described in Iran: *A. persicus* ($K2P > 9$) (Mahmoudi et al., 2020). Nuclear and mitochondrial data support the specific status of these two species (Mahmoudi et al., 2020).

The Italian lineage is the most differentiated within *A. amphibius* s.l. ($K2P \geq 4.4$). Reproductive isolation has been evidenced between animals from the north and south sides of the Swiss Alps, populations that can be nowadays attributed to the Western European L1 and the Italian L4 (Morel, 1979) in (Castiglia et al., 2016)). This supports the Italian lineage as an incipient species: *A. italicus* (type locality Pisa, Italy).

The other lineages (Western European L1, Eurasiatic L2, and Turkish L3) correspond partially to entities that have been even recently proposed as separate species: *A. amphibius* and *A. monticola* (Mahmoudi et al., 2020). In Mahmoudi et al. (2020), *A. monticola* was proposed for fossorial voles from Western Europe (Switzerland and Spain), which are included in our Lineage 1, whereas *A. amphibius* include Siberian (aquatic) and European (aquatic and fossorial) voles, which are included in our Lineage 2. The genetic divergence between lineages 1, 2, and 3 was rather low ($K2P = 2.9\text{--}4.1$), hence they are most likely phylogenetic lineages related to repeated isolations in glacial refugia during the Quaternary climatic fluctuations (Michaux, Chevret, Filippucci, & Macholan, 2002; Taberlet, Fumagalli, Wust-Saucy, & Cosson, 1998). Furthermore, our extensive sampling evidenced that the two main lineages (1 and 2) can co-occur in the same localities at the fringe of their respective distribution area. In the population of Chapelle d'Huin, (Doubs, France), showing a co-occurrence of lineages 1 and 2, specimens display a skull shape typical of L1. This suggests that exchanges between the two lineages occur at the nuclear level. The three lineages, which present low genetic divergence, should thus be attributed to a single species: *A. amphibius* (Linnaeus, 1758) (including the former recognized species *amphibius*, *monticola*, *sherman*, and *terrestris*).

ACKNOWLEDGEMENTS

The authors are deeply indebted to all contributors who provided samples from the different regions, or helped in the preparation of the material: E. Aarnink, H. Ansoerge, T. Asferg, K. Baumann, S. Blome, T. Büchner, P. Callesen, J. Caspar, F. Catzeflis, F. Chanudet, J.-F. Cosson, G. Couval, C. Crespe, M. Debussche, the Derek Gow Consultancy Ltd, S. Drewes, H. Dybdahl, A. Globig, J.-D. Graf, B. Hammerschmidt, A. Hellemann, H. Henttonen, J. Huitu, J. Jacob, D. Kaufmann, N. Kratzmann, C. Kretzschmar, V. Kristensen, E. Krogh Pedersen, J. Lang, P. Lestrade, D. Maaz, C. Maresch, C. Martins, A. Meylan, J. Morel, E. Perreau, K. Plifke, B. Pradier, F. Raoul, D. Reil, S. Reinholdt, U. M. Rosenfeld, M. Ruedi, T. Ruys, M. Schlegel, S. Schmidt, T. Schröder, J. Schröter, H. Sheikh Ali, N. Stieger, J. Struyck, J. Thiel, F. Thomas, D. Truchetet, J.R. Vericad, G. Villadsen, K. Wanka, U. Wessels, A. Wiehe, D. Windolph, R. Wolf, T. Wollny, I. Yderlisere. M.P. Bournonville is particularly thanked for her participation to the acquisition of the genetic data. This work was performed using the computing facilities of the CC LBBE/PRABI. Johan Michaux benefited from FRS-FNRS grants ("directeur de recherches"). The sequencing of the *cytochrome b* gene was performed using private funding from the Conservation Genetics Laboratory of the University of Liège. We thank the anonymous reviewers for their constructive comments.

ORCID

Pascale Chevret  <https://orcid.org/0000-0002-4186-875X>
 Sabrina Renaud  <https://orcid.org/0000-0002-8730-3113>
 Zeycan Helvacı  <https://orcid.org/0000-0002-1793-7460>
 Rainer G. Ulrich  <https://orcid.org/0000-0002-5620-1528>
 Johan R. Michaux  <https://orcid.org/0000-0003-4644-9244>

REFERENCES

- Adams, D. C., & Otárola-Castillo, E. (2013). geomorph: An R package for the collection and analysis of geometric morphometric shape data. *Methods in Ecology and Evolution*, 4(4), 393–399. <https://doi.org/10.1111/2041-210X.12035>
- Adams, D. C., Rohlf, F. J., & Slice, D. E. (2013). A field comes of age: Geometric morphometrics in the 21st century. *Hystrix, the Italian Journal of Mammalogy*, 24, 7–14.
- Akaike, H. (1973). Information theory as an extension of the maximum likelihood principle. In B. N. Petrov & F. Csaki (Eds.), *Second international symposium on information theory* (pp. 267–281). Budapest, Hungary: Akademiai Kiado. <https://doi.org/10.2307/2334537>
- Amori, G., Gippoliti, S., & Castiglia, R. (2009). European non-volant mammal diversity: Conservation priorities inferred from phylogeographic studies. *Folia Zoologica*, 58(3), 270–278.
- Bandelt, H. J., Forster, P., & Rohl, A. (1999). Median-joining networks for inferring intraspecific phylogenies. *Molecular Biology and Evolution*, 16(1), 37–48. <https://doi.org/10.1093/oxfordjournals.molbev.a026036>
- Barbosa, S., Pauperio, J., Searle, J. B., & Alves, P. C. (2013). Genetic identification of Iberian rodent species using both mitochondrial and nuclear loci: Application to noninvasive sampling. *Molecular Ecology Resources*, 13(1), 43–56. <https://doi.org/10.1111/1755-0998.12024>
- Bookstein, F. L. (1997). Landmark methods for forms without landmarks: Morphometrics of group differences in outline shape. *Medical Image Analysis*, 1(3), 225–243. [https://doi.org/10.1016/S1361-8415\(97\)85012-8](https://doi.org/10.1016/S1361-8415(97)85012-8)

- Brace, S., Ruddy, M., Miller, R., Schreve, D. C., Stewart, J. R., & Barnes, I. (2016). The colonization history of British water vole (*Arvicola amphibius* (Linnaeus, 1758)): Origins and development of the Celtic fringe. *Proceedings of the Royal Society B: Biological Sciences*, 283, 20160130. <https://doi.org/10.1098/rspb.2016.0130>
- Bryja, J., Mikula, O., Šumbera, R., Meheretu, Y., Aghová, T., Lavrenchenko, L. A., ... Verheyen, E. (2014). Pan-African phylogeny of *Mus* (subgenus *Nannomys*) reveals one of the most successful mammal radiations in Africa. *BMC Evolutionary Biology*, 14(1), 256. <https://doi.org/10.1186/s12862-014-0256-2>
- Castiglia, R., Aloise, G., Amori, G., Annesi, F., Bertolino, S., Capizzi, D., ... Colangelo, P. (2016). The Italian peninsula hosts a divergent mtDNA lineage of the water vole, *Arvicola amphibius* s.l., including fossorial and aquatic ecotypes. *Hystrix, the Italian Journal of Mammalogy*, 27(2). <https://doi.org/10.4404/hystrix-27.2-11588>
- Cubo, J., Ventura, J., & Casinos, A. (2006). A heterochronic interpretation of the origin of digging adaptations in the northern water vole, *Arvicola terrestris* (Rodentia: Arvicolidae). *Biological Journal of the Linnean Society*, 87(3), 381–391. <https://doi.org/10.1111/j.1095-8312.2006.00575.x>
- Darriba, D., Taboada, G. L., Doallo, R., & Posada, D. (2012). jModelTest 2: More models, new heuristics and parallel computing. *Nature Methods*, 9(8), 772–772. <https://doi.org/10.1038/nmeth.2109>
- Durão, A. F., Ventura, J., & Muñoz-Muñoz, F. (2019). Comparative post-weaning ontogeny of the mandible in fossorial and semi-aquatic water voles. *Mammalian Biology*, 97, 95–103. <https://doi.org/10.1016/j.mambio.2019.05.004>
- Gomes Rodrigues, H., Šumbera, R., & Hautier, L. (2016). Life in burrows channelled the morphological evolution of the skull in rodents: The case of African mole-rats (Bathyergidae, Rodentia). *Journal of Mammalian Evolution*, 23(2), 175–189. <https://doi.org/10.1007/s10914-015-9305-x>
- Gouy, M., Guindon, S., Gascuel, O., & Lyon, D. (2010). SeaView version 4: A multiplatform graphical user interface for sequence alignment and phylogenetic tree building. *Molecular Biology and Evolution*, 27(2), 221–224. <https://doi.org/10.1093/molbev/msp259>
- Guindon, S., Dufayard, J.-F., Lefort, V., Anisimova, M., Hordijk, W., & Gascuel, O. (2010). New algorithms and methods to estimate maximum-likelihood phylogenies: assessing the performance of PhyML 3.0. *Systematic Biology*, 59(3), 307–321. <https://doi.org/10.1093/sysbio/syq010>
- Heim de Balsac, H., & Guislain, R. (1955). Évolution et spéciation des campagnols du genre *Arvicola* en territoire français. *Mammalia*, 19(3), 367–390. <https://doi.org/10.1515/mamm.1955.19.3.367>
- Kohli, B. A., Speer, K. A., Kilpatrick, C. W., Batsaikhan, N., Damdinbaza, D., & Cook, J. A. (2014). Multilocus systematics and non-punctuated evolution of Holarctic Myodini (Rodentia: Arvicolinae). *Molecular Phylogenetics and Evolution*, 76, 18–29. <https://doi.org/10.1016/j.ympev.2014.02.019>
- Kryštufek, B., Koren, T., Engelberger, S., Horváth, G. F., Purger, J. J., Arslan, A., ... Murariu, D. (2015). Fossorial morphotype does not make a species in water voles. *Mammalia*, 79(3), 293–303. <https://doi.org/10.1515/mammalia-2014-0059>
- Kumar, S., Stecher, G., & Tamura, K. (2016). MEGA7: Molecular evolutionary genetics analysis version 7.0 for bigger datasets. *Molecular Biology and Evolution*, 33(7), 1870–1874. <https://doi.org/10.1093/molbev/msw054>
- Leigh, J. W., & Bryant, D. (2015). POPART: Full-feature software for haplotype network construction. *Methods in Ecology and Evolution*, 6(9), 1110–1116. <https://doi.org/10.1111/2041-210X.12410>
- Mahmoudi, A., Maul, L. C., Khoshyar, M., Darvish, J., Aliabadian, M., & Kryštufek, B. (2020). Evolutionary history of water voles revisited: Confronting a new phylogenetic model from molecular data with the fossil record. *Mammalia*, 84(2), 171–184. <https://doi.org/10.1515/mammalia-2018-0178>
- Michaux, J. R., Chevret, P., Filippucci, M.-G., & Macholan, M. (2002). Phylogeny of the genus *Apodemus* with a special emphasis on the subgenus *Sylvaemus* using the nuclear IRBP gene and two mitochondrial markers: *Cytochrome b* and 12S rRNA. *Molecular Phylogenetics and Evolution*, 23(2), 123–136. [https://doi.org/10.1016/S1055-7903\(02\)00007-6](https://doi.org/10.1016/S1055-7903(02)00007-6)
- Michaux, J., Chevret, P., & Renaud, S. (2007). Morphological diversity of Old World rats and mice (Rodentia, Muridae) mandible in relation with phylogeny and adaptation. *Journal of Zoological Systematics and Evolutionary Research*, 45(3), 263–279. <https://doi.org/10.1111/j.1439-0469.2006.00390.x>
- Michaux, J. R., Magnanou, E., Paradis, E., Nieberding, C., & Libois, R. (2003). Mitochondrial phylogeography of the Woodmouse (*Apodemus sylvaticus*) in the Western Palearctic region. *Molecular Ecology*, 12(3), 685–697.
- Miller, W., Schuster, S. C., Welch, A. J., Ratan, A., Bedoya-Reina, O. C., Zhao, F., ... Lindqvist, C. (2012). Polar and brown bear genomes reveal ancient admixture and demographic footprints of past climate change. *Proceedings of the National Academy of Sciences of the United States of America*, 109(36), E2382–E2390. <https://doi.org/10.1073/pnas.1210506109>
- Montgelard, C., Bentz, S., Tirard, C., Verneau, O., & Catzeflis, F. M. (2002). Molecular systematics of sciurognathi (rodentia): The mitochondrial *cytochrome b* and 12S rRNA genes support the Anomaluroidea (Pedetidae and Anomaluridae). *Molecular Phylogenetics and Evolution*, 22(2), 220–233. <https://doi.org/10.1006/mpev.2001.1056>
- Morel, J. (1979). *Le campagnol terrestre en Suisse: Biologie et systématique (Mammalia Rodentia)*. Lausanne, Switzerland: Université de Lausanne.
- Mouton, A., Mortelliti, A., Grill, A., Sara, M., Kryštufek, B., Juškaitis, R., ... Michaux, J. R. (2017). Evolutionary history and species delimitations: A case study of the hazel dormouse, *Muscardinus avellanarius*. *Conservation Genetics*, 18(1), 181–196. <https://doi.org/10.1007/s10592-016-0892-8>
- Pardiñas, U., Ruelas, D., Bradley, L., Bradley, R., Ordóñez, N., Kryštufek, B., ... Brito, M. J. (2017). Cricetidae (true hamsters, voles, lemmings and new world rats and mice) - Species accounts of Cricetidae. In D. Wilson, T. E. J. Lacher & R. A. Mittermeier (Eds.), *Handbook of the mammals of the world. Volume 7. Rodents II* (pp. 280–535). Barcelona, Spain: Lynx Edici.
- Paupério, J., Herman, J. S., Melo-Ferreira, J., Jaarola, M., Alves, P. C., & Searle, J. B. (2012). Cryptic speciation in the field vole: A multilocus approach confirms three highly divergent lineages in Eurasia. *Molecular Ecology*, 21(24), 6015–6032. <https://doi.org/10.1111/mec.12024>
- Rambaut, A. (2012). *FigTree v1.4*. Retrieved from <https://github.com/rambaut/figtree/releases>
- Rambaut, A., Suchard, M. A., Xie, D., & Drummond, A. J. (2014). *Tracer v1.6*. Retrieved from <http://beast.bio.ed.ac.uk/Tracer>
- Renaud, S., Dufour, A.-B., Hardouin, E. A., Ledevin, R., & Auffray, J.-C. (2015). Once upon multivariate analyses: When they tell several stories about biological evolution. *PLoS ONE*, 10(7), e0132801.
- Renaud, S., Hardouin, E. A., Quéré, J. P., & Chevret, P. (2017). Morphometric variations at an ecological scale: Seasonal and local variations in feral and commensal house mice. *Mammalian Biology*, 87, 1–12. <https://doi.org/10.1016/j.mambio.2017.04.004>
- Rohlf, F. J. (2010). *Tpsdig v.2. Ver. 2.16: Ecology and evolution*. Stony Brook, NY: SUNY.
- Rohlf, F. J., & Slice, D. (1990). Extensions of the Procrustes Method for the Optimal Superimposition of Landmarks. *Systematic Biology*, 39(1), 40–59.
- Ronquist, F., Teslenko, M., van der Mark, P., Ayres, D. L., Darling, A., Höhna, S., ... Huelsenbeck, J. P. (2012). MrBayes 3.2: Efficient Bayesian phylogenetic inference and model choice across a large model space. *Systematic Biology*, 61(3), 539–542. <https://doi.org/10.1093/sysbio/sys029>

- Rozas, J., Ferrer-Mata, A., Sánchez-DelBarrio, J. C., Guirao-Rico, S., Librado, P., Ramos-Onsins, S. E., & Sánchez-Gracia, A. (2017). DnaSP 6: DNA sequence polymorphism analysis of large data sets. *Molecular Biology and Evolution*, 34(12), 3299–3302. <https://doi.org/10.1093/molbev/msx248>
- Samuels, J. X., & Van Valkenburgh, B. (2009). Craniodental adaptations for digging in extinct burrowing beavers. *Journal of Vertebrate Paleontology*, 29(1), 254–268.
- Schlager, S. (2017). Morpho and Rvcg - Shape analysis in R. In G. Zheng, S. Li & G. Székely (Eds.), *Statistical shape and deformation analysis* (pp. 217–256). Cambridge, MA: Academic Press.
- Searle, J. B., Kotlík, P., Rambau, R. V., Marková, S., Herman, J. S., & McDevitt, A. D. (2009). The Celtic fringe of Britain: Insights from small mammal phylogeography. *Proceedings. Biological Sciences/The Royal Society*, 276(1677), 4287–4294. <https://doi.org/10.1098/rspb.2009.1422>
- Taberlet, P., Fumagalli, L., Wust-Saucy, A. G., & Cosson, J.-F. (1998). Comparative phylogeography and postglacial colonization routes in Europe. *Molecular Ecology*, 7(4), 453–464.
- Vallejo, R. M., & González-Cózar, F. X. (2012). Phylogenetic affinities and species limits within the genus *Megadontomys* (Rodentia: Cricetidae) based on mitochondrial sequence data. *Journal of Zoological Systematics and Evolutionary Research*, 50(1), 67–75. <https://doi.org/10.1111/j.1439-0469.2011.00634.x>
- Ventura, J., & Casado-Cruz, M. (2011). Post-weaning ontogeny of the mandible in fossorial water voles: Ecological and evolutionary implications. *Acta Zoologica*, 92(1), 12–20. <https://doi.org/10.1111/j.1463-6395.2010.00449.x>
- Wilson, D. E., & Reeder, D. M. (Eds.) (1993). *Mammals species of the world, a taxonomic and geographic reference* (2nd ed.). Washington, DC: Smithsonian.
- Wilson, D. E., & Reeder, D. M. (Eds.) (2005). *Mammal species of the world* (3rd ed.). Baltimore, MD: The Johns Hopkins University Press.
- Wust-Saucy, A. G. (1998). *Polymorphisme génétique et phylogéographie du campagnol terrestre Arvicola terrestris*. Lausanne, Switzerland: Université de Lausanne.

Alignment S1. Alignments of *cytochrome b* sequences used in the present study.

Figure S1. Examples of water vole skulls in ventral and lateral view, with the location of the landmarks (red dots) and sliding semi-landmarks (blue dots along the black lines).

Figure S2. Phylogenetic tree reconstructed with the *cytochrome b* mitochondrial gene. For the main nodes, the support is indicated as follow: posterior probability (MrBayes)/bootstrap support (PhyML). The different lineages are indicated on the right side of the phylogeny. The color code of the sequence names represents the ecology: in orange fossorial; in blue aquatic.

Table S1. Sampling for the genetic study. JPQ, Jean-Pierre Quéré; JRM, Johan R. Michaux; RGU, Rainer G. Ulrich.

Table S2. Sampling for the morphometric study. GxE, grouping variable combining genetics and ecology. Nventral/Nlateral: number of skulls measured in ventral/lateral view. CBGP, Centre de Biologie et Gestion des Populations (Baillarguet, Paris); JPQ, Jean-Pierre Quéré; JRM, Johan R. Michaux; MHN, Muséum d'Histoire Naturelle (Geneva, Switzerland); ULG, Université de Liège (Belgium).

How to cite this article: Chevret P, Renaud S, Helvacı Z, Ulrich RG, Quéré J-P, Michaux JR. Genetic structure, ecological versatility, and skull shape differentiation in *Arvicola* water voles (Rodentia, Cricetidae). *J Zool Syst Evol Res*. 2020;00:1–12. <https://doi.org/10.1111/jzs.12384>

SUPPORTING INFORMATION

Additional supporting information may be found online in the Supporting Information section at the end of the article.